Building and Environment 163 (2019) 106242

Contents lists available at ScienceDirect

Building and Environment

journal homepage: www.elsevier.com/locate/buildenv

High albedo materials to counteract heat waves in cities: An assessment of meteorology, buildings energy needs and pedestrian thermal comfort

Serena Falasca[a,b,*], Virgilio Ciancio[c], Ferdinando Salata[c], Iacopo Golasi[c], Federica Rosso[d], Gabriele Curci[b,e]

[a] Department of Pure and Applied Sciences (DISPeA), University of Urbino, 61029, Urbino, Italy
[b] Center of Excellence in Telesensing of Environment and Model Prediction of Severe Events (CETEMPS), University of L'Aquila, 67100, L'Aquila, Italy
[c] Department of Astronautical, Electrical and Energy Engineering - Area Fisica Tecnica, University of Rome "Sapienza", Via Eudossiana 18, 00184, Rome, Italy
[d] Department of Civil, Construction and Environmental Engineering (DICEA), University of Rome "Sapienza", Via Eudossiana 18, 00184, Roma, Italy
[e] Department of Physical and Chemical Sciences (DSFC), University of L'Aquila, 67100, L'Aquila, Italy

ARTICLE INFO

Keywords:
Heat wave
Urban heat island
High albedo materials
WRF
Energy needs
Outdoor thermal comfort

ABSTRACT

Climatological data show that the frequency of Heat Waves (HWs) has increased since the 1950s and that it will continue to increase. These phenomena exasperate the urban heat island (UHI) phenomenon. In this study, we investigated the impact of a HW on the UHI in Milan (Italy); we also analyzed the effects of the application of high albedo materials on the vertical and horizontal urban built surfaces. We performed numerical experiments with the Weather Research and Forecasting model, whose output were used as input for the EnergyPlus software and the computation of the Mediterranean Outdoor Comfort Index (MOCI). Our results showed that the HW induces a maximum increase of about 4 °C in the temperature at 2 m height and that the use of high albedo materials covering all urban surfaces only partially counteracts this increase. The wind speed decreases due to the HW and the introduction of high albedo materials leads to its further decrease. The cooling energy consumption for a building located in the city doubles in the presence of HW and high albedo materials have a negligible positive effect when applied to the surrounding urban environment. The HW brings an increase up to about 0.7 of the MOCI and the use of high albedo materials further worsens thermal sensation. Therefore, this mitigation strategy leads to considerable benefits in terms of temperature and energy, while it determines a penalization of the well-being of the pedestrian. Its application requires a careful evaluation of benefits and side effects.

1. Introduction

Climate warning is leading to the intensification of extreme weather events such as heavy precipitation, floods, droughts, and heat waves [1]. A heat wave (HW) is generally defined as a period of abnormally and uncomfortably hot weather, but a single and universally accepted definition is currently not available and rather a set of indices based on extreme temperatures or on the number of hot days exists [2,3]. The frequency of HWs has increased since 1950 in different parts of Europe, Asia and Australia, and their frequency and duration are expected to increase [1].

The harmful effects that ever more frequent HWs have on the quality of life are now recognized, both in terms of direct effects linked to high temperatures (e.g. harmful for health, thermal comfort, energy consumption) and of indirect effects (e.g. increased pollution). HWs exacerbate thermal stresses that particularly influence the inhabitants of big cities, which are already affected by the phenomenon of the Urban Heat Island (UHI), which is the heating of urban areas compared to the surrounding suburbs [4]. Many studies have been conducted to quantify such thermal stresses around the world. For example, in the residential area of the Seoul mega city the maximum values of the Physiological Subjective Temperature (PST) [5] were found between 44.1 °C and 54.0 °C during the heat wave of 2016 [6]. During significant heat wave events, the Physiological Equivalent Temperature (PET) reached values higher than 40 °C in Novi Sad (Serbia) and in Iran [7,8]. Also, the acclimatization is affected by HWs and pedestrians feel warmer, even with the same values of Universal Thermal Climate Index (UTCI) of no-HW periods. Salata et al. [9] analyzed aspects related to

* Corresponding author. Department of Pure and Applied Sciences (DISPeA), University of Urbino, Campus Scientifico Enrico Mattei, 61029 Urbino, PU, Italy.
E-mail addresses: serena.falasca@uniurb.it (S. Falasca), virgilio.ciancio@uniroma1.it (V. Ciancio), ferdinando.salata@uniroma1.it (F. Salata), iacopo.golasi@uniroma1.it (I. Golasi), federica.rosso@uniroma1.it (F. Rosso), gabriele.curci@aquila.infn.it (G. Curci).

https://doi.org/10.1016/j.buildenv.2019.106242
Received 9 May 2019; Received in revised form 20 June 2019; Accepted 1 July 2019
Available online 02 July 2019
0360-1323/

acclimatization and adaptation in the Mediterranean area. Their results showed that pedestrians modify their thermal clothing insulation in case of intense thermal stresses, such as those associated with UHIs or HWs. The importance of urban design in the warm months to limit the discomforts of thermal perception caused by intense heat conditions is highlighted by Tseliou et al. [10] in their study on Athens (Greece). Cohen et al. [11] examined the human thermal perception in Tel Aviv (Israel), where the UHI intensity in summer reaches 2.2 °C. In particular, they observed that the PET scale should take into account also the seasonal climatic variations.

The effects of the simultaneous presence of UHIs and HWs recently started to receive scholarly attention. Founda and Santamouris [12] found an intensification of the average UHI magnitude by up to 3.5 °C during HW episodes in the extremely hot summer of 2012 in Athens, compared to summer background conditions. Ramamurthy and Sangobanwo [13] showed that during extreme heat days the UHI was amplified in most of the ten US cities considered in their study. D'Ippoliti et al. [14] found that the climatic events occurred in Rome between 1992 and 2004 caused a 28.8% increase of natural deaths of people older than 60 years.

Numerical studies showed synergies between HWs and UHIs which intensify the difference between urban and rural temperatures [15,16]. Ward et al. [17] revealed that factors like the regional climate, the fraction of soil sealing, and the presence of water bodies are influencing factors during HWs more than the population size, with cooler northern European cities resulting to be more vulnerable to HWs than southern European cities.

During a HW, also buildings located in a city centre are subjected to a further thermal load in addition to that due to the UHI [18]. Evins et al. [19] estimated that the greater energy exchanges due to long wave radiation lead to an increase in air temperatures of about 6 °C with a growth of energy needs of more than 20%. When external temperature reaches values higher than the project temperature of the air conditioning systems [20], there is an anomalous energy demand [21]. Therefore, if correctly sized, during a HW air conditioning systems are brought to the maximum service conditions without being able to comply with the required indoor comfort conditions. On the contrary, if oversized the systems can continue to guarantee the internal comfort conditions, with a significant increase in energy consumption compared to periods of less intense heat. Some Authors quantified such increases in the energy demand of buildings in Italian and European cities. For example, Savić et al. [22] found an increment of the energy demand equal to 0.15 MW for the city of Somber (Serbia). Two scientific works demonstrated that in central Italy (cities of Modena and Perugia), buildings in the city center have 10% more energy consumption than buildings in rural areas due to the UHI, and that this energy consumption increases by 351% during extremely hot summer periods [23,24]. Hence, mitigating the urban microclimate by implementing appropriate countermeasures can prevent an extraordinary energy demand for cooling buildings and an overload of the plants with consequent problematic operating conditions [25].

Despite the wide scientific evidence, the mechanisms underlying the interaction between UHIs and HWs are not entirely clear [26] and Ramamurthy and Sangobanwo [13] emphasized the need for localized analysis taking into account local processes and dynamics (e.g. sea breeze or coastal winds) in the characterization of UHIs variability. In this context, we focus on the UHI of Milan, which is the second most populous city in Italy and is located south of the Alps in the river Po valley, Northern Italy. Here, local dynamics linked to the action of slope winds play a key role, as shown by Falasca and Curci [27]. The UHI of Milan has been diagnosed and extensively studied also using satellite data [27]. Furthermore the epidemiologic study by Conti et al. [28] showed that the increase in mortality during the summer 2003 was 30.6% in Milan.

Mitigation measures of UHIs consist of architectural techniques applied to the built environment aimed at reducing ambient and surface temperatures by altering the local surface energy balance. Implementation of mitigation strategies are crucial also for the urban microclimate in order to relieve the thermal perception of pedestrians which is quantified by means of suitable indexes, for example the Mediterranean Outdoor Comfort Index (MOCI) developed by Salata et al. [29] with the aim of predicting the thermo-hygrometric perception of the Mediterranean population.

Highly reflective materials, cool and green roofs, urban greening are those architectural strategies that have attracted more attention. Several studies showed their effectiveness in mitigating urban high temperatures [30–33]. Zhang et al. [34] proved that increasing the roof albedo to 0.5 and 0.7 has a similar effectiveness as 25% and 50% of green roof coverage, respectively. In some conditions and types of cities, the strongest cooling effect can be achieved by combining mitigation strategies with benefits both on urban macroclimate and microclimate [35–37]. In particular, in their study on the campus of Sapienza University of Rome Salata et al. [38] found that the joint use of cool roofs, cool pavements and an increase in urban vegetation lead to an average decrease in air temperature of about 1.49 °C and of the MOCI [29] of about 0.24 units. Furthermore, Salata et al. [37,39] showed that on a hot summer day the application of high albedo materials instead of cobblestones on the basic surface of the yard leads to an increase in Predicted Mean Vote (PMV) [40] of about 1 unit and to an increase in PMV of about 2 units if the high albedo materials are applied also to the walls.

Other mitigation strategies are analyzed in the literature, such as cool pavements, insulating materials inside the walls, air conditioning systems not directly ejecting into the atmosphere [41,42]. Akbari et al. [43] provided a review on the state of the art in the field of UHI mitigation strategies. Moreover, the effect UHI mitigation techniques on urban ambient temperature establishes a virtuous cycle, because both cooling energy demand [44] and pollutants emissions [45] are reduced.

As UHI mitigating actions alter the local surface energy balance, they also affect the local meteorology and the structure of the planetary boundary layer [46], specifically involving stagnation of air near the surface and potentially causing air quality degradation [27,47].

In this study, we aim at identifying the effects of the 10-day HW occurred during July 2015 in Milan on the circulation of the local UHI, on the local meteorology, on the energy needs for cooling a hypothetical building and on the local outdoor thermal comfort. The effect of using highly reflective materials to cover urban surfaces on these topics are also investigated in order to evaluate benefits and side effects of this UHI mitigation measure. To this end, we apply the WRF model at high resolution (~1 km) and outputs are provided as input to the EnergyPlus software for the evaluation of buildings cooling energy demand and for the computation of the Mediterranean Outdoor Comfort Index for the evaluation of the pedestrian thermal perception.

2. Materials and methods

The employed method is described in this section and in greater detail in the next subsections. As our aim is to identify the effects of the considered HW phenomenon on UHI, on energy needs and on outdoor thermal comfort, we employ a meteorological model for the assessment of the meteorological urban field of Milan (described in section 2.1). We then consider the surface energy balance to identify the influencing variables to modify in our model (section 2.2) and define the simulation scenarios and time periods (section 2.3). In order to characterize the scenarios so as to be as more realistic as possible, we conduct a careful analysis of the albedo values to insert in the simulation (section 2.4). Finally, we conduct an analysis of the energy needs of a building located inside the urban area (2.5) and of the outdoor thermal comfort in the urban area (2.6).

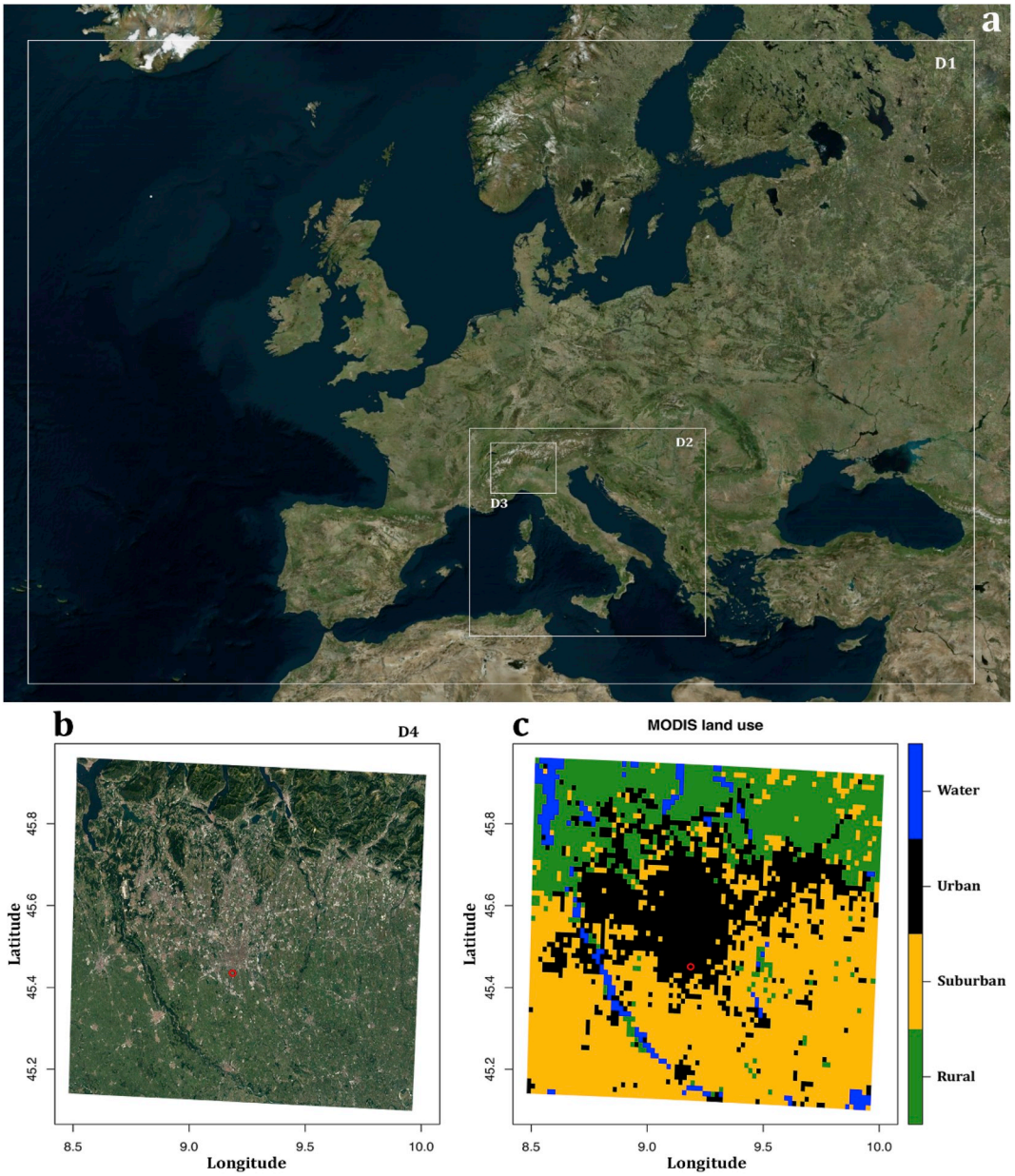

Fig. 1. Properties of the model domains: (a) Geographical areas covered by the four nested domains; (b) innermost domain; (c) land use categories (from MODIS) in the innermost domain. The suburban area corresponds to the "croplands" category and the rural area corresponds to the "mixed forests" category. The red circle in (b) and (c) denotes the position of the building simulated with EnergyPlus and of the Bocconi weather station. More information on the four domains are in Table 1.

2.1. The meteorological model

We employ a mesoscale numerical weather prediction tool, the WRF model (version 3.7.1) [48], to simulate meteorological fields over Milan. The four nested domains are shown in Fig. 1a and b, with the outermost domain covering Europe (Fig. 1a) and the innermost domain (Fig. 1b) covering the metropolitan area of Milan (Northern Italy). Fig. 1c shows the MODIS land-use of the domain over Milan, where the "Urban", "Suburban" and "Rural" labels are assigned to the urban, croplands and mixed forests land use categories respectively. WRF domains are regular in terms of distance in km (a Lambertian projection is used) with the horizontal grid size decreasing (with a ratio equal to 4) from 36 km of the European domain to 1.3 km of the domain over Milan (Table 1). Physics options used are summarized in Table 2, with the multi-layer Building Environment Parameterization (BEP) [49] chosen as the urban physics option with default values for input thermal and morphological parameters. In this work, the BEP scheme uses the same value of parameters for the three types of urban texture (commercial, high residential, low residential), since the MODIS dataset includes only one urban category. More details on the WRF configuration are provided in the previous paper by Falasca and Curci [50].

Table 1
Configuration of the WRF domains.

Domain	Geographical Area	Resolution (km)	Number of grid cells (long x lat)
D1	Europe	36	108 × 102
D1	Italy	12	102 × 108
D3	North-Western Italy	4	93 × 93
D4	Milan	1.333	84 × 66

Table 2
Labels and description of numerical experiments.

Label	Scenario	Year	Albedo		
			Roofs	Streets	Walls
no-HW	Base case	2014	0.2	0.2	0.2
HW	Heat Wave (HW)	2015	0.2	0.2	0.2
HW-R	HW with high-albedo roofs only	2015	0.7	0.2	0.2
HW-Tot	HW with high-albedo all surfaces	2015	0.7	0.7	0.7

2.2. The surface energy balance

According to Oke [51], neglecting the net heat advection the surface energy balance (SEB) equation reads:

$$Q^* + Q_F = Q_H + Q_E + \Delta Q_S \quad (1)$$

Where:

- Q^* is the net all-wave radiation flux density;
- Q_F is the anthropogenic heat flux density due to combustion;
- Q_H and Q_E are the turbulent flux densities of sensible and latent heat, respectively;
- ΔQ_S is the net heat storage.

The net all-wave radiation, Q^*, is computed as follows:

$$Q^* = R_{SW}\downarrow - R_{SW}\uparrow + R_{LW}\downarrow - R_{LW}\uparrow \quad (2)$$

where:

- $R_{SW}\downarrow$ is the incident short wave radiation,
- $R_{SW}\uparrow$ is the upward short-wave radiation and is computed as $R_{SW}\uparrow = \alpha R_{SW}\downarrow$ where α is the albedo coefficient and indicates the reflection of incoming solar radiation from a certain surface,
- $R_{LW}\downarrow$ is the incident long wave radiation,
- $R_{LW}\uparrow$ is the upward long wave radiation and is computed as $R_{LW}\uparrow = \varepsilon\sigma T_0^4$ where ε is the surface thermal emissivity (the capacity to emit thermal radiation), $\sigma = 5.67040 \cdot 10^{-8}$ $Js^{-1}m^{-2}K^{-4}$ is the Stefan–Boltzmann constant and T_0 is the surface skin temperature.

2.3. Simulation scenarios and time periods

In order to elucidate the role of the HW, we considered two simulation periods: 14–23 July 2014 and 14–23 July 2015. On the basis of an exploratory analysis of the daily temperatures in Milan in the years between 2012 and 2016, 2015 resulted an exceptionally hot year and 2014 a cool year on average compared to other years. The period 14–23 July was chosen because it was characterized by the most important HW in the summer 2015. For the no-HW period (2014) we considered only the base case, characterized by default values of albedo (equal to 0.2) for all urban surfaces (roofs, roads and walls), while for the HW period we defined three simulation scenarios (Table 2): (1) the base case, characterized by default values of albedo (equal to 0.2) for all urban surfaces (roofs, roads and walls); (2) the intermediate mitigation test case, characterized by a high value of albedo (equal to 0.7) only for roofs; (3) the extreme mitigation test case, characterized by a high value of albedo (equal to 0.7) for roofs, roads and walls.

We performed four runs with WRF corresponding to the four scenarios described in Table 2 and meteorological fields computed by WRF were extracted in correspondence of the red dot in Fig. 1 and then used to build suitable weather files for EnergyPlus (Section 2.5) and as input for the computation of the MOCI (Section 2.6).

2.4. High-albedo materials choice

In Section 2.2, the importance of albedo (α) in the equation of net all-wave radiation for the $R_{SW}\uparrow$ term is highlighted. Albedo defines the reflection of incoming solar radiation from a certain surface and can be calculated as the ratio of radiosity (the radiant flux from a surface) and irradiance (the incoming radiant flux on that surface). Very often in literature on high albedo materials, solar reflectance is also considered as an indicator of albedo: highly reflective materials are high albedo materials. In Ref. [52], both solar reflectance and albedo are measured in field on the same materials. The effectiveness of high albedo/highly reflective materials in mitigating UHI is due to the reflection of solar radiation, that does not heat up urban surfaces. On the other hand, low albedo and low reflective materials absorb solar radiation, and are responsible of higher surface and air temperatures. Doulos and colleagues [53] and Alchapar and colleagues [54] performed comprehensive experimental analyses of a large variety of materials (more than 40) employed in urban areas. They highlighted the role of light-colored and smooth materials, classified as cool materials, in maintaining lower surface temperatures, with respect to dark-colored and rough materials.

In this work we are considering the entire urban surface, divided into its main components, i.e., streets, roofs, and vertical envelope (walls). The need to assume one unique value for each of these surfaces, e.g., one for all the streets, one for all the roofs and one for all the envelopes, requires careful considerations, given the large variety of possible urban materials with different albedo values. Indeed, this work aims at highlighting the effect of high albedo materials at a macro, urban scale: while it was not possible to differentiate materials' albedo within the same surface category (e.g., street) in the same scenario (described in section 2.3), the albedo values that are employed were selected after careful consideration.

The main material for the streets is asphalt, which has very low albedo, even if it slightly increases as time passes. The reported values for asphalt are between 0.12 and 0.24 albedo [55,56]. We considered also that many streets are composed by asphalt roads but concrete or other similar paving material as sidewalk. With reference to Refs. [54,56], concrete tiles possess an albedo close to 0.30. Therefore, as a mean of the gathered values, we considered albedo 0.2 for the streets (Table 2).

For the roof, both the case of tiled roof, typical of many historical city centers, and bitumen membranes, which are very common in the Italian building stock of the later XX century, where taken into account in defining the albedo values of roof surface category. Studies reported experimentally measured values of 0.19 for historical roof tiles [57,58], while for bitumen roofs albedo values comprised between 0.13 and 0.2 are reported [59]. However, there are also paved roof, for which we considered generic tiles and concrete tiles, i.e., albedo around 0.3. Therefore, also for roof urban surfaces the value 0.2 for albedo was employed, so as to mediate the above reported values.

With respect to the vertical envelope, a wider difference exists among possible materials' albedo, given the architectural variety of the envelope system. Indeed, in Italian cities we can find massive, plastered, brick or stone envelopes built before the XXI century, as well as glass, stone, PVC or metal facades typical of the last decades. Considering that reddish-grayish plasters have albedo equal to 0.2–0.3, darker stone or concrete prefabricated panels 0.2 [60], we selected the value of 0.2 for the non-cool scenarios (Table 2).

For the "cool" version of urban surfaces, characterizing the urban scenarios that exploit high-albedo materials, the literature reports quite homogenous values for cool surfaces, generally comprised between 0.6 and 0.8. Therefore, we selected albedo equal to 0.7 for both streets, roofs and envelopes, as a mean value among the gathered ones. Indeed, high-albedo materials exist in a wide variety of colors and possible base-materials but are all characterized by high albedo and high solar reflectance values. Not only light-colored ones but also dark-colored cool materials have been developed recently, exploiting the infrared part of the solar spectrum instead of the visible part of the spectrum [60–62].

2.5. The analysis of energy needs

For the analysis of the energy needs of the building taken as reference, we used the EnergyPlus energy simulation software. Developed by the Department of Energy (DOE) of the U.S. and by the Building Technologies Office (BTO), EnergyPlus is based on the most popular features of BLAST and DOE-2. It allows to perform energy simulations of residential buildings in dynamic regime [63,64], and to analyze the energy demands of the building. Unlike BLAST and DOE-2, EnergyPlus uses detailed and refined algorithms in the simulation process, and for this reason it is a point of reference for the international scientific community to calculate the energy needs of buildings [65]. EnergyPlus includes manifold simulation functions, such as the possibility to set the time steps of the simulation and to size the heating and cooling systems based on the design internal well-being conditions defined by the designer. Depending on the site chosen for the simulation it is possible to use the weather data available on EnergyPlus site, including over 2,100 locations (of which 1,042 in the United States, 71 in Canada and over 1,000 in 100 countries worldwide) [66].

As a case study building to be employed as a reference building (Fig. 2) in the numerical analyses, in this work, the simulations were carried out considering a building whose ground floor consists partially in a pilotis plan. The building is residential type and it consists of three stories, in addition to the ground floor employed as a technical room. In each story there are three apartments, with different surface development to examine the influence of different families on energy consumption. The connection system consists of a staircase, equipped with a lift which leads the occupants from the ground floor to the upper floors, and a walkway for each floor that leads to the entrance of the apartments. The roof of the building has a flat extension, which makes it usable partly by the inhabitants and partly for future installations of passive solar systems. Each floor has an internal surface extension of 320.4 m^2, with a height of 2.8 m (from the floor); the heated surface, without the connection system, is equal to 261.2 m^2 per floor, with a total of 783.24 m^2 for the whole building.

The thermal load due to the period studied in the simulations (July 14th - July 23rd) is treated by the installation of direct expansion split systems (COP = 3.1) for each apartment. The ventilation of the interiors is supposed to be natural with a rate of air changes equal to 0.5 hour volume.

As already described in section 2.3, the weather files used as input for the EnergyPlus software are built using the meteorological fields produced by WRF for the four scenarios in Table 2. The meteorological variables provided as provided as output by WRF and used as input to EnergyPlus are: dry bulb temperature, dew point temperature, relative humidity, atmospheric pressure, wind speed and wind direction [75]. In addition, for the HW-R and HW-Tot scenarios two more simulations were performed with EnergyPlus, changing the albedo value of roof and of roof and walls of the building, respectively. In this way, it was possible to investigate how the energy consumption of the building varies not only when the external weather conditions (the city surrounding the building) change, but also when the albedo of the building itself changes.

2.6. Outdoor thermal comfort

In order to carry out the analysis of the thermal perception of pedestrians in the different scenarios considered in this work (Table 2), the micrometeorological conditions in the red dot in Fig. 1b are examined. This analysis is based on the MOCI [29] and weather variables

Fig. 2. Three-dimensional (3D) model and plan of a standard floor of the analyzed building.

needed for its computation are obtained from the WRF outputs. The original configuration of the MOCI included air temperature, average radiant temperature, wind speed, relative humidity and thermal clothing insulation as independent variables. On the other side, in this study the mean radiant temperature is not available while the global radiation is one of the fields provided by WRF runs. For this reason, using the thermal perception votes and the corresponding values of the micrometeorological variables sampled by Salata et al. [29], the following relation for MOCI was obtained:

$$MOCI = -4.257 + 0.325 \cdot I_{CL} + 0.146 \cdot T_A + 0.005 \cdot RH + 0.001 \cdot I_S - 0.235 \cdot WS \quad (3)$$

where:

- I_{CL} is the thermal clothing insulation;
- T_A is the ambient temperature (provided by WRF);
- RH is the relative humidity (provided by WRF);
- I_S the total incident radiation (provided by WRF);
- WS is the wind speed intensity (provided by WRF).

Concerning the regression statistics, an adjusted R^2 value of 0.37 was obtained, a R^2 value of 0.38 and a Pearson coefficient of 0.609.

The values of the thermal clothing insulation to be included in the Equation (3) of the MOCI are strictly related to mechanisms such as adaptation, acclimatization and thermal expectation and are computed from Equation (4), that has been experimentally derived from the data sampled by Salata et al. in Ref. [67]:

$$I_{CL} = 1.608 - 0.038 \cdot T_A \quad (4)$$

Finally, note that the MOCI is based on a symmetrical scale of seven values. This scale goes from −3 to +3, with extreme values representing a very cold and very hot thermal perception respectively, and with the zero value representing the condition of thermal neutrality.

3. Evaluation of the Weather Research and Forecasting model

Outputs of the Weather Research and Forecasting model (WRF) were evaluated for both the no-HW and HW cases. Temperature and wind speed were interpolated and then extracted at the geographical coordinates of the "Bocconi" weather station of the ClimateNetwork® of Osservatorio Milano Duomo (OMD) Foundation, where also the building simulated by EnergyPlus is located and where the outdoor thermal comfort of pedestrians was evaluated. The "Bocconi" weather station is located at a height of 30.6 m from the ground, with a total altitude of 144.6 m. Fig. 3 shows the comparison between the mean daily cycles of temperature and wind speed computed by the WRF model and the values acquired by the "Bocconi" weather station and Table 3 shows a statistical summary (fractional bias, normalized mean square error, correlation coefficient, and the fraction of modeled values within a factor of two of observations) of the comparison. In the Supplementary material, the comparison between observations and model is provided for the mean daily cycles averaged for seven stations of the ClimateNetwork® of OMD Foundation all over the urban area of Milan (Figs. 1S and 2S, Table 1S).

As discussed in Ref. [50], the model is able to reproduce correctly the daily temperature cycle, with practically negligible bias values in the afternoon and an underestimation of a few degrees Celsius during

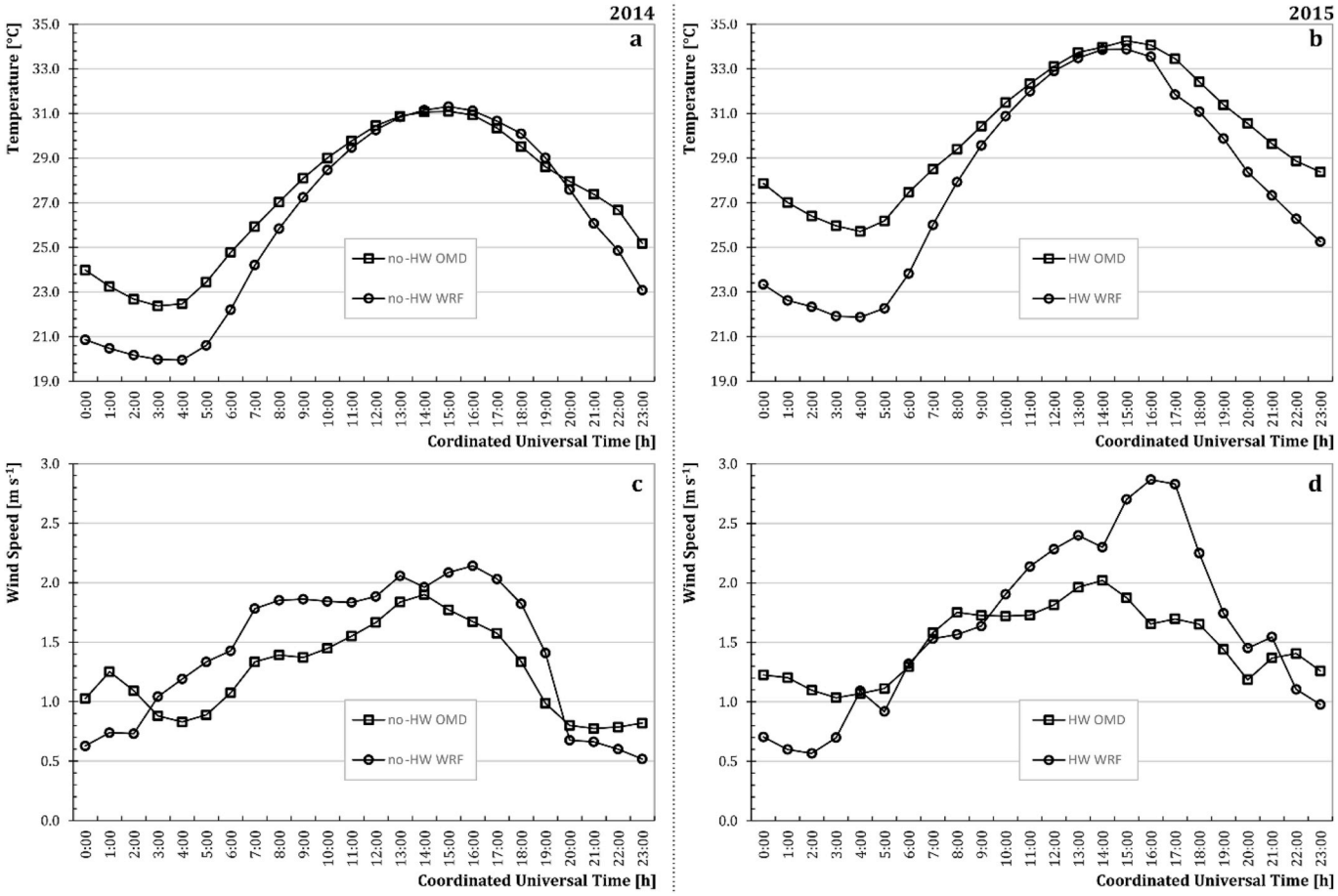

Fig. 3. Mean daily cycles of temperature (a, b) and wind speed (c, d) as computed by the WRF model and acquired by the "Bocconi" weather station for non-Heat Wave and Heat Wave scenarios.

Table 3
Statistical parameters of the comparison between observations and model at the "Bicocca" weather station for temperature and wind speed and non-Heat Wave and Heat Wave scenarios.

	HW		no-HW	
	Temperature	Wind Speed	Temperature	Wind Speed
Fractional Bias (FB)	−0.00653	−0.1078	−0.00452	−0.0296
Normalized Mean Square Error (NMSE)	$8.1161 \cdot 10^{-5}$	0.2351	$5.0990 \cdot 10^{-5}$	0.1449
Correlation Coefficient (R)	0.931	0.483	0.938	0.639
Fraction of predictions within a factor of two of observations (FAC2)	1	0.744	1	0.859

the night (fractional bias equal to −0.00452 in 2014 and -0.00653 in 2015). The bias between modeled and observed temperature during nighttime, especially over urban areas, is a well-known issue in the atmospheric modeling and is an open issue in the field (e.g. Refs. [68–70]). Also, with regard to wind speed, the model overestimates the speed intensity especially during the night with values of the fractional bias equal to −0.0296 in 2014 and -0.1078 in 2015. Overall, the bias between model and observations in the no-HW and HW cases is such that the average hourly temperature difference between the HW and no-HW scenarios is practically negligible in the central hours of the day and is underestimated by the model of maximum 1.5 °C in the evening (Fig. 4a). On the contrary, the HW- no-HW wind speed difference is underestimated by the model during the morning (maximum ~1 m/s) and overestimated in the afternoon. Based on these observations, we believe that the model thus configured is appropriate for this study.

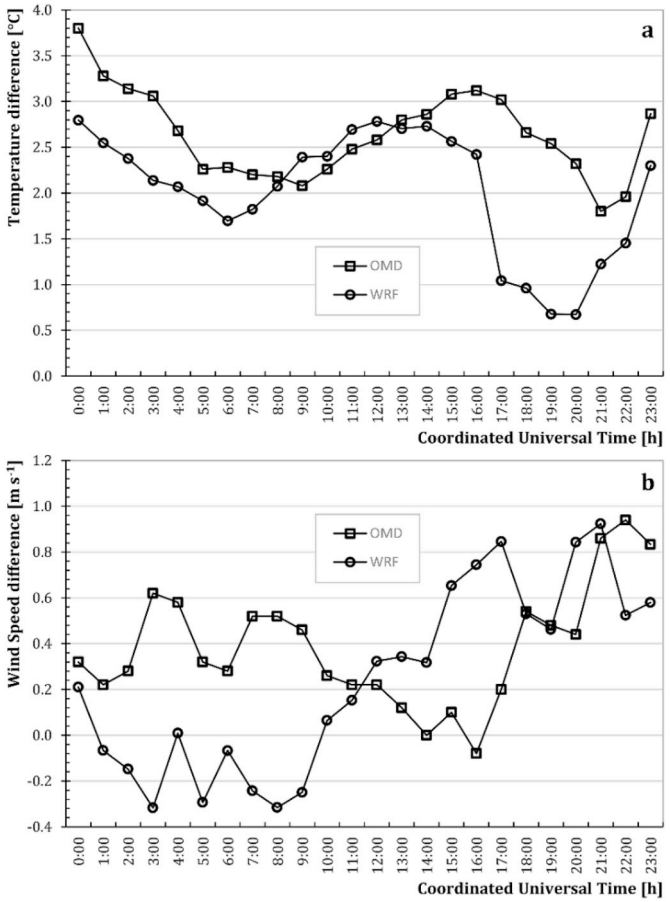

Fig. 4. Daily cycles of the observed and modeled difference between HW and no-HW cases for: a) temperature, b) wind speed.

4. Results and discussion

We illustrate and discuss here the results of the numerical experiments described in section 2.3 and in Table 2. Results are split in three subsections: the first one is focused on the meteorological variables temperature and wind speed, the second one is focused on the energy and power consumption for cooling the building and the third one is focused on the outdoor thermal comfort. Note that the "Urban", "Suburban" and "Rural" labels are assigned to the urban, croplands and mixed forests land use categories respectively.

4.1. Meteorology

During the HW period the temperature at 2 m (T2m) is higher than in 2014 on the whole domain over Milan both at 00:00 LT and at 12:00 LT, with up to 4.5 °C of difference at 00:00 LT (Fig. 5). At night, there is a spatial heterogeneity in the HW - no-HW T2m difference (hereinafter HW - no-HW ΔT2m) among the land use categories, and also the daily cycle of HW - no-HW ΔT2m depends on the land use (Fig. 6). In fact, at night the suburban and rural areas have very similar behavior and they display higher differences with respect to the urban area, while during daytime the temperature difference is more uniform. The HW - no-HW ΔT2m varies from a minimum of 2.7 °C at night to a maximum of 3.9 °C in the evening in the urban area and from 3 °C at noon to 3.6 °C in the evening in non-urban areas (Fig. 6a); in terms of percentage these differences are from 12% to 20% (Fig. 6b). The reduced day-night percentage difference in the urban area is a sign of the UHI effect. The UHI intensity is defined as the temperature difference between the urban and a surrounding area and at night it is about 3 °C, while during the day is about 1 °C (not shown). During the HW period, rural and suburban areas heat up more than the urban area at night, thus the resulting UHI intensity is reduced by half degree with respect to the no-HW period.

Another fundamental meteorological variable for the characterization of the circulation associated with the UHI is the horizontal wind speed at 10 m height (W10 m). W10 m is generally lower in the presence of HW on almost all the domain and throughout the day (Fig. 5c and d and Fig. 6c and d), with a maximum difference of about −0.5 m/s (−30%) in the central part of the day (Fig. 6c and d). The nighttime reduction of HW - no-HW ΔW10 m could be due to the lowering of the UHI intensity compared to no-HW period. As also noted in Ref. [27], the urban – non-urban W10 m difference is generally negative because of the higher surface roughness in the city than in the surroundings. During the HW period, however, the sign of the difference is reversed in the central part of the day, meaning that the HW reduces wind speeds more effectively in the surroundings of the urban area.

Among the existing mitigation techniques, high albedo materials are taken into consideration in this work and here we want to investigate the effectiveness of this technique with respect to the heat wave. As described in Section 2, these materials are applied only on urban surfaces, therefore they affect marginally non-urban areas. In this

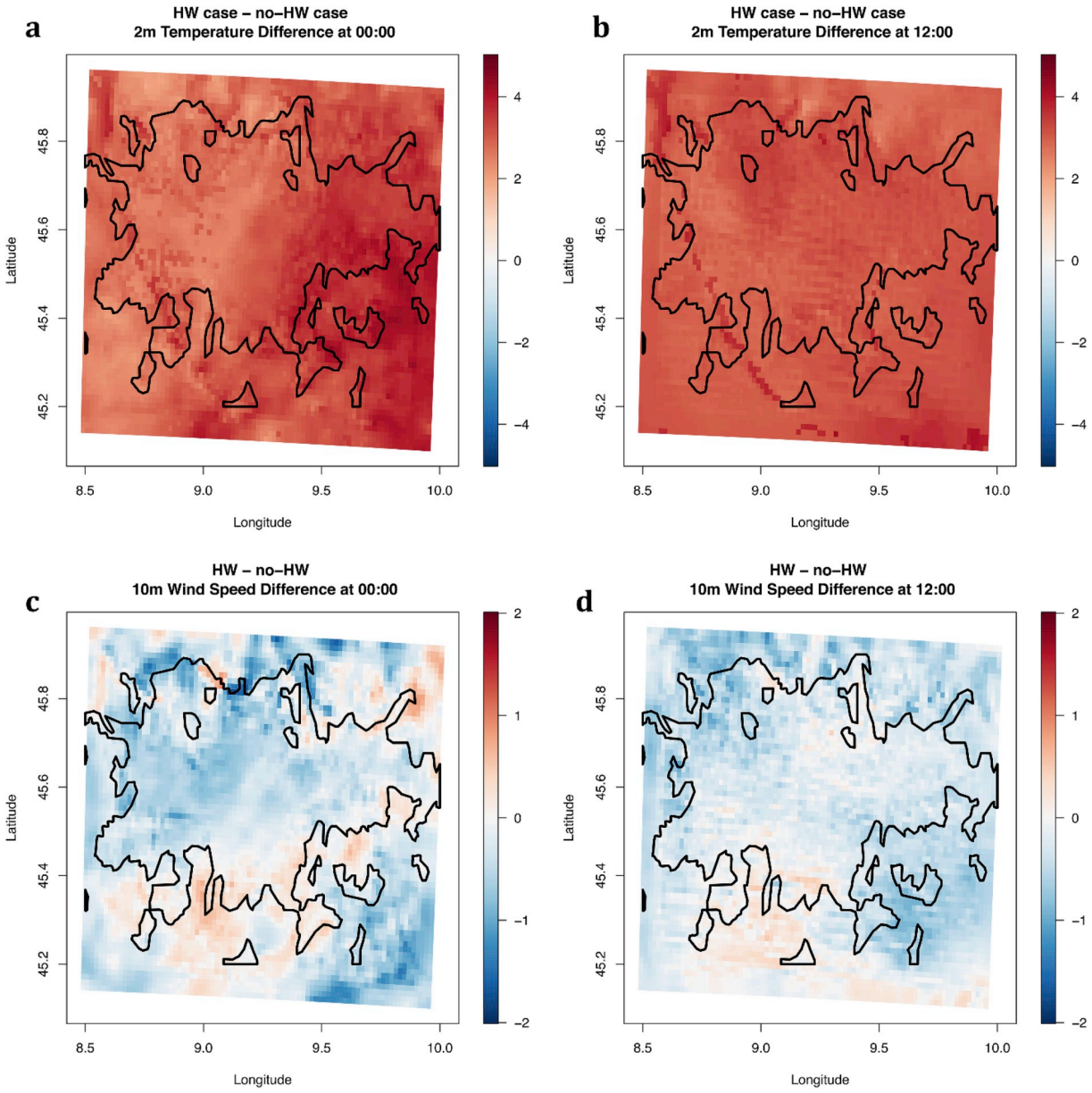

Fig. 5. Maps of the mean 2 m temperature (a, b) and 10 m Wind Speed (c, d) difference between HW and no-HW cases in the innermost domain at 00:00 LT and 12:00 LT. The black thick line indicates the boundary of the metropolitan area of Milan as derived from the MODIS satellite data [71].

subsection only results concerning the urban area discussed, while daily cycles of temperature and wind speed averaged over the rural and suburban areas are shown in the supplementary material. As specified in Sections 2.2 and 2.4, albedo represents the reflected fraction of the incident shortwave radiation, therefore it influences directly the corresponding term in the surface energy balance equation and, indirectly, the other terms of the surface energy balance. Fig. 7a and b shows that during the HW period (year 2015), thanks to the mitigation measure T2m is reduced over the whole domain considered and, as expected, to a greater extent on the urban area. In fact, T2m is also slightly reduced in suburban and rural areas, although the mitigation technique is applied only the urban area. Moreover, the benefit of this technique extends also to the night, even if it primarily acts on the reflected solar radiation. In a previous study, [27] showed that high albedo materials are effective in reducing the ambient temperature in the urban area of Milan also during the relatively cool summer period of 2014. Here, we show that the mean benefit deriving from the use of highly reflective materials is similar in the presence and in the absence of HW. Indeed, both in 2014 and in 2015 the extreme case presents negative values of UHI intensity during the morning; furthermore, UHI intensities in 2014 and 2015 are similar because the HW determines an almost uniform heating over both urban and non-urban areas (not shown). Furthermore, although in the HW-Tot case the T2m is lower than that of the HW case (by about 2 °C), it still remains higher than in the no-HW case (Fig. 8a). The high albedo materials may thus help mitigating the thermal discomfort due to HW, but they are not able to reduce temperatures to those comparable with no-HW periods.

Fig. 8 shows that W10 m decreases in HW-R and even more in HW-

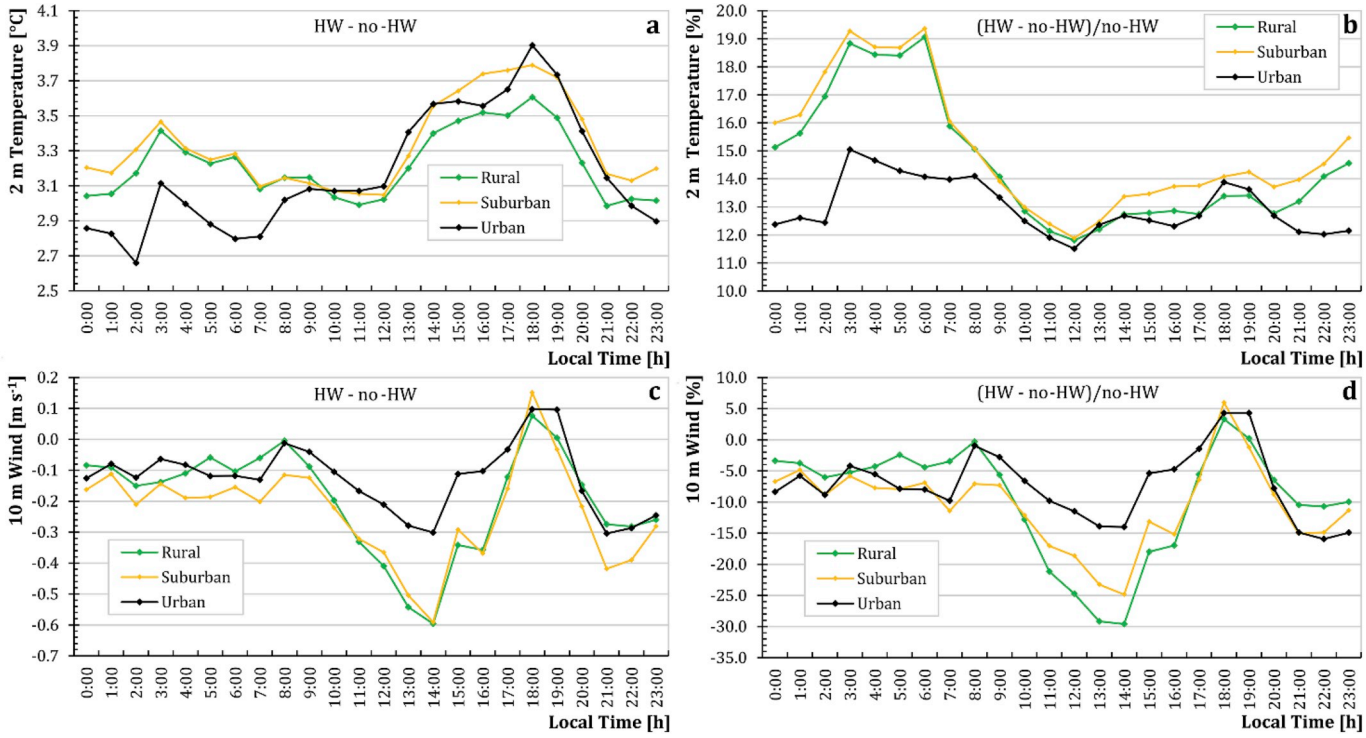

Fig. 6. Daily cycles of: (a) 2 m Temperature (°C) and (c) 10 m Wind Speed (m/s) difference between 2015 and 2014 averaged over the simulation period (14–23 July) for the Reference case and the Urban (black line), Suburban (yellow line) and Rural (green line) cells; (b and d) Same as (a and c), but as a percentage difference with respect to 2014 temperature and wind speed.

Tot compared to the HW case, so much that the difference between urban areas and non-urban areas has negative values during the entire daily cycle. The application of high albedo materials determines the reduction of W10 m, progressively in HW-R and HW-Tot. From the spatial point of view the impact of these materials is practically uniform (Fig. 7c and d), while from the temporal point of view the difference between the extreme case HW-Tot and the reference case HW increases progressively during the day's hours reaching a maximum value of about 1 m/s.

4.2. Energy needs

As described in section 2.5, simulations were carried out with EnergyPlus using as input the weather data provided by WRF runs for the scenarios simulated (HW, HW-R and HW-Tot cases) without altering the values of the building's albedo. Furthermore, for the HW-R and HW-Tot scenarios, further simulations were carried out modifying the albedo values of the surfaces of the building studied.

Thanks to these simulations, it was possible to quantify the following effects of high albedo materials on the energy demand: i) the mitigation of air temperatures within the city; ii) the increase of the solar radiation reflection from the surfaces of the building analyzed towards outside. The first effect involves external weather conditions more favorable and, therefore, lower energy consumption. In addition, there is a decrease in the thermal load of the building considered and therefore a decrease in its energy needs for cooling. In this section, the incidence of each of these effects on the global needs for cooling the case study building has been quantified.

Fig. 9 shows in gray the values of the variables (energy demand, peak power and median power) normalized with respect to the "no-HW" case. For the HW-R and HW-Tot cases, the white bar also shows the value of each variable if only the external weather conditions were modified, keeping the albedo value of the building surfaces constant. In fact, the numbers on the top of the white bars indicate the consumption of the building studied computed with the simulations in which the building albedo is kept constant. On the other side, the numbers on the top of the gray bars indicate the values of the quantities obtained with the simulations in which also the albedo on the surfaces of the studied building is changed.

In Fig. 9, the median takes into account the time frequency of the hourly power and is representative of consumptions because the higher this value is, more energy will be required in the target period. On the other side, the peak power fails to provide useful indications from an energy point of view since even if it assumes a high value, it is for a short time. Normalized energy (Fig. 9a) increases almost by 100% in the HW case compared to the no-HW case. In the HW-R case, the energy demand drops by 1% thanks to the use of high albedo materials in the urban area and by 62% when high albedo materials are applied also to the studied building. This effect is even more marked if high albedo materials are used on all urban surfaces: the reduction of the air temperature involves a 5% decrease in the needs that are reduced even to 96% compared to the no-HW case.

Similar considerations can be made for the peak power. In the HW case, the peak power increases by 30% compared to the no-HW case and this could constitute an operational problem if the plants have not been oversized to cope with a similar climatic event since they could be inadequate in the period of highest demand for summer air conditioning. Such power peaks do not vary if the effects of high albedo materials on the city weather are considered (both HW-R and HW-Tot), but they decrease if the presence of such materials is simulated on the surfaces of the studied building, up to cancel the effect of the presence of the HW (Fig. 9b).

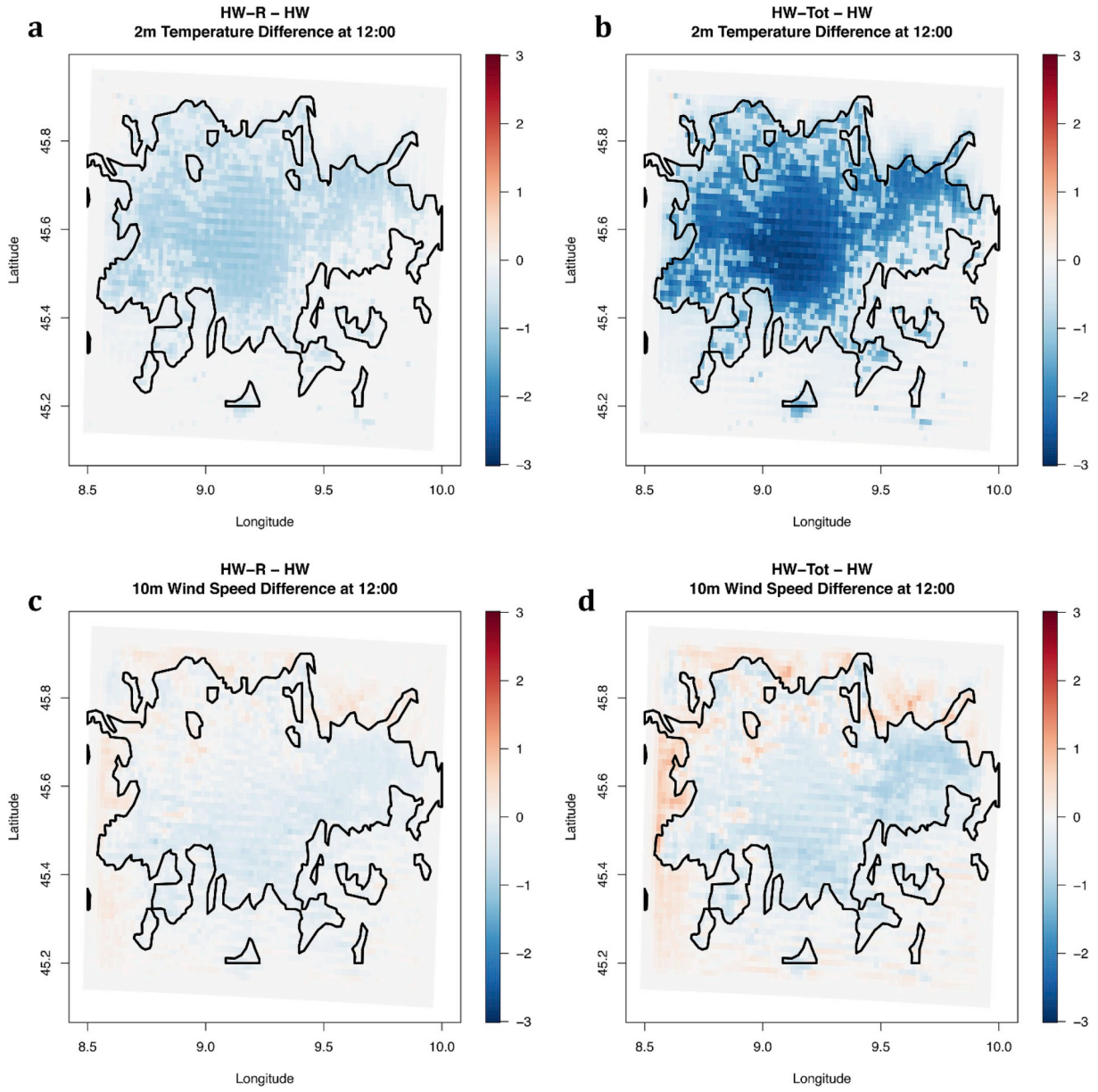

Fig. 7. Maps of the mean 2 m temperature (a, b) and 10 m Wind Speed (c, d) difference between the test cases (HW-R and HW-Tot) and the reference case HW in the innermost domain at 12:00 LT. The black thick line indicates the boundary of the metropolitan area of Milan as derived from the MODIS satellite data [71].

The median of hourly power has an even more marked trend than the power. Indeed, the HW-Tot scenario is characterized by a lower value of the median than the no-HW scenario (Fig. 9c).

4.3. Outdoor thermal comfort

In order to evaluate the effect of the Heat Wave on the thermo-hygrometric perception of pedestrians, the Mediterranean Outdoor Comfort Index (MOCI) was calculated. As mentioned in Section 2.5, it was calculated at the same location of the building simulated with EnergyPlus (red dot in Fig. 1b) and Fig. 9 illustrates its trend for the four scenarios analyzed (no-HW, HW, HW-R, HW-Tot) during an average day. It shows that the Heat Wave leads to a general increase in the MOCI, which reaches 0.7 units during the central hours of the day.

This is a consequence of the higher values of air temperatures, up to 4 °C higher during the hottest hours of the day in presence of Heat Wave. In this regard, it should be highlighted that the air temperature has been identified as the variable mostly influencing the outdoor thermal comfort [72,73]. The differences between values of the MOCI in presence and in absence of the Heat Wave are then equal to about 0.5 units even during the evening and the night and reach their minimum during the first hours of the morning.

Concerning the influence of high albedo materials on outdoor thermal comfort, Fig. 10 shows that the implementation of cool roofs does not lead to significant variations. In fact, the major deviations with respect to the HW case are about 0.2 units in terms of MOCI. A possible explanation could lie in the height of the buildings in the simulated area. It is in fact generally higher than 30 m and this leads to a decrease in the influence of this mitigation strategy at the pedestrians level. Similar results have been found by Wang et al. [42] in the city of Toronto in Canada.

A worsening of the microclimate is instead detected in the case in which the high albedo materials are applied on all surfaces (HW-Tot case). In this case, in fact, they also appear on surfaces characterized by a reduced sky view factor, such as roads and especially walls. This leads to the establishment of multiple inter-reflections and a consequent

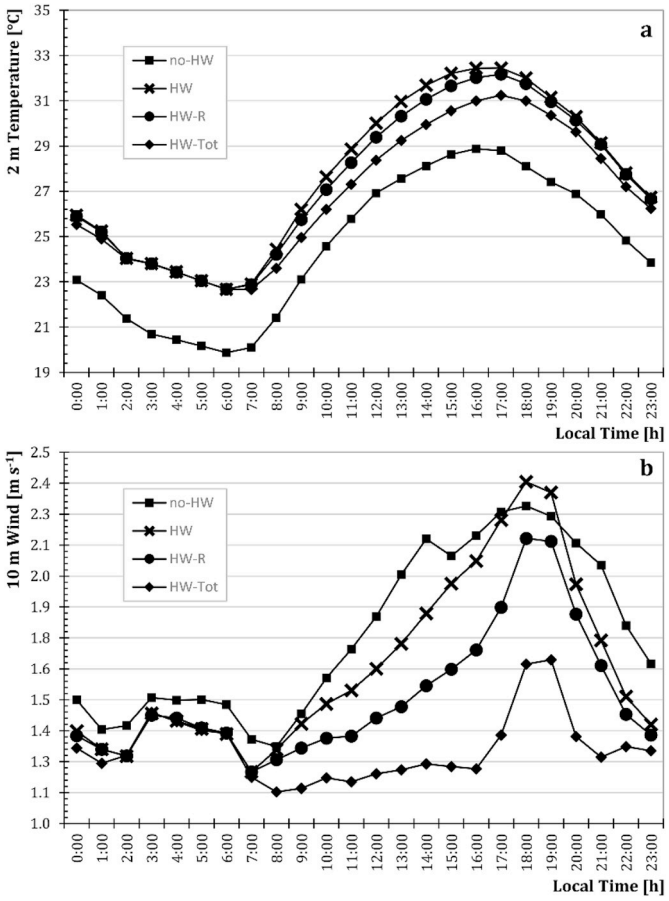

Fig. 8. Daily cycles of (a) 2 m temperature and (b) 10 m wind speed averaged over the urban area for the base case in 2014 and the three simulation scenarios in 2015.

increase in micrometeorological variables such as average radiant temperatures and air temperatures. To be more detailed, these changes lead to an increase in the MOCI that in the afternoon hours can even reach 0.45 units. Also the progressive decrease of wind speed intensity in HW-R and HW-Tot cases, discussed in Section 4.1 and shown in Fig. 8, contribute to the increase of the MOCI under these scenarios.

Furthermore, Fig. 10 shows that in the hours when there is no strong

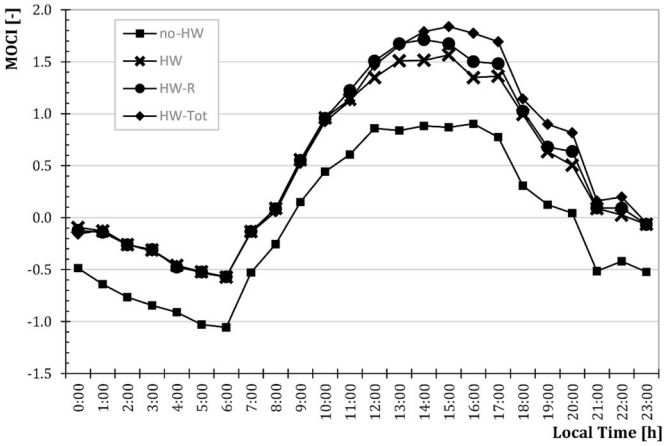

Fig. 10. Trend of the Mediterranean Outdoor Comfort Index (MOCI) for the base case in 2014 (no-HW) and the three simulation scenarios in 2015 (HW, HW-R, HW-Tot).

solar radiation, high albedo materials do not provide significant variations in thermal comfort sensations (expressed with MOCI) compared to the HW scenario.

5. Conclusions

Heat waves (HWs) are extreme weather events whose frequency has increased since the middle of the last century. This trend is not expected to decrease, therefore the knowledge of the repercussions that these phenomena have on lives of people, now living to a greater extent in large cities, is crucial. In this work we studied the impact of a HW on the properties of the UHI in Milan (Northern Italy). We also investigated the HW impact on the energy needs for cooling a reference building and on outdoor thermal comfort of pedestrians in the same city. To this end, we performed numerical experiments using the WRF model over the metropolitan area of Milan in the periods 14–23 July 2014 and 14–23 July 2015 and the outputs of WRF runs were used as input for the dynamical energy simulations through the EnergyPlus software and for the evaluation of the Mediterranean Outdoor Comfort Index (MOCI).

The two years were chosen as representative of a heat wave (HW) and non-heat wave (no-HW) period and runs were designed appropriately. For the no-HW scenario only a base case was considered,

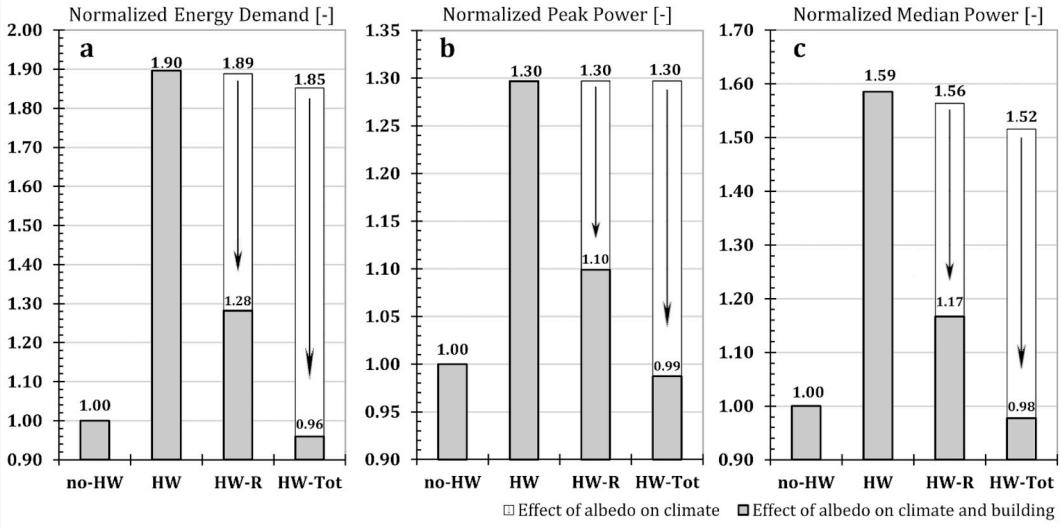

Fig. 9. Normalized energy demand [kWh] (a), normalized peak power [kW] (b) and normalized median power [kW] (c) for the analyzed building.

characterized by the same albedo value for roofs, walls and streets of the urban area and equal to the default value of 0.2 in the WRF model; for the HW period, two tests cases were considered besides the base case: a case with a high value of albedo (equal to 0.7) only for the roofs and a case with a high albedo value (equal to 0.7) for all urban surfaces.

The comparison of time series of 2 m temperature (T2m) in absence and in presence of the HW shows that rural and suburban areas heat up more than the urban area during the night, but the T2m difference during the daily cycle has a greater variation in the urban area compared to the non-urban ones, implying that the urban area is more sensitive and vulnerable to the HW. We found that the nighttime UHI intensity is lower in the presence of HW, while during the day the effect is less pronounced. The horizontal wind speed (W10 m) is lower in the presence of HW than in its absence throughout the day, and to a greater extent during the central hours of the day and in non-urban areas. The use of high albedo materials in the presence of HW leads to a reduction of the ambient temperature in the urban area of Milan and its effectiveness is not compromised by the presence of the HW. Nevertheless, the use of these materials is not sufficient to cancel the effect of the HW.

The energy demand in the considered building doubles in the HW case with respect to the no-HW case and the introduction of high albedo materials in the surrounding urban environment reduces it maximum by 5% in the HW-Tot scenario. The application of high-albedo materials on the building itself brings a significant reduction in energy demand, up to balance the effect of the HW. The peak and median powers are less affected by the presence of the HW than the energy demand, but in the same way as the energy, they decrease significantly only if the high albedo materials are applied also to the building itself.

The use of high albedo materials allows obtaining important energy savings for the analyzed building and, for transitive properties, for all buildings in the city. However, this mitigation strategy is not an advantageous solution from the point of view of thermal comfort for pedestrians. Indeed, in the HW-R case and even more in the extreme case HW-Tot the values of MOCI increase in the central hours of the day since there is a greater reflection of solar radiation. The MOCI index rises towards values that are too high for the Mediterranean normotype.

All these considerations lead to the conclusion that urban planning taking into account the use of high albedo materials as a HWs mitigation strategy must necessarily include a careful evaluation of thermal, economic and environmental benefits and of the collateral effects, such as pedestrian well-being.

Future studies could take into account the coupled employment of green and high-albedo materials cooling strategies to further cool down urban areas in the hot season and in particular in the occurrence of heat-waves. Moreover, in addition to considering thermal comfort, the visual comfort should be taken into account when applying cool materials at the city scale: indeed, studies demonstrated the deleterious effect, in terms of visual comfort, of such bright and highly-reflective materials [52]. The use of dark-colored but cool materials and green solutions could mitigate such issue.

We also considered crucial for studies on urban areas to introduce improvements in the WRF numerical set-up by using more detailed databases of land use in the urban environment. The application of the World Urban Database and Access Portal Tools (WUDAPT) database, for example, which includes ten categories of urban land use is an example of possible improvement.

Funding

This research did not receive any specific grant from funding agencies in the public, commercial, or not-for-profit sectors. In particular, Ferdinando Salata gratefully acknowledges Sapienza University of Rome for the support deriving from the grant "Progetti di Ricerca - Progetti Medi 2018".

Acknowledgments

The computational resources for WRF runs were provided by CINECA in the framework of the Iscra-C project ALTARIS7. We acknowledge the CINECA award under the ISCRA initiative, for the availability of high performance computing resources and support. We also acknowledge Osservatorio Milano Duomo (OMD) Foundation for providing observations of the ClimateNetwork® stations. Serena Falasca would like to acknowledge Prof. Umberto Giostra (University of Urbino) for the helpful discussions.

Appendix A

Statistical parameters used to compare model to observations are defined as follows [74]:

Fractional bias (FB)

$$FB = \frac{(\overline{C_o} - \overline{C_p})}{0.5(\overline{C_o} + \overline{C_p})} \tag{5}$$

- Normalized mean square error (NMSE):

$$NMSE = \frac{\overline{(C_o - C_p)^2}}{\overline{C_o}\ \overline{C_p}} \tag{6}$$

- Correlation coefficient (R):

$$R = \frac{\overline{(C_o - \overline{C_o})(C_p - \overline{C_p})}}{\sigma_{C_p}\sigma_{C_o}} \tag{7}$$

- Fraction of modelled values within a faction of two of observations (FAC2):

$$0.5 \leq \frac{C_p}{C_o} \leq 2.0 \tag{8}$$

where:

- C_p represents modelled values;

- C_o represents observed values;
- overbar $\bar{C}$ represents average over dataset;
- σ_C represents the standard deviation over the dataset.

Appendix A. Supplementary data

Supplementary data to this article can be found online at https://doi.org/10.1016/j.buildenv.2019.106242.

References

[1] AR5 Climate Change 2013, The Physical Science Basis — IPCC (n.d.), https://www.ipcc.ch/report/ar5/wg1/ , Accessed date: 8 February 2019.

[2] L.V. Alexander, X. Zhang, T.C. Peterson, J. Caesar, B. Gleason, A.M.G. Klein Tank, M. Haylock, D. Collins, B. Trewin, F. Rahimzadeh, A. Tagipour, K. Rupa Kumar, J. Revadekar, G. Griffiths, L. Vincent, D.B. Stephenson, J. Burn, E. Aguilar, M. Brunet, M. Taylor, M. New, P. Zhai, M. Rusticucci, J.L. Vazquez-Aguirre, Global observed changes in daily climate extremes of temperature and precipitation, J. Geophys. Res. Atmos. 111 (2006) 1–22, https://doi.org/10.1029/2005JD006290.

[3] D. a Collins, N. Plummer, B.C. Trewin, Trends in annual frequencies of, Aust. Meteorol. Mag. 49 (2000) 277–292.

[4] F. Chen, X. Yang, W. Zhu, WRF simulations of urban heat island under hot-weather synoptic conditions: the case study of Hangzhou City, China, Atmos. Res. 138 (2014) 364–377, https://doi.org/10.1016/j.atmosres.2013.12.005.

[5] K. Blazejczyk, The Updated Version of Man-Environment Heat Exchange Model, (2005).

[6] M.K. Hwang, J.H. Bang, S. Kim, Y.K. Kim, I. Oh, Estimation of thermal comfort felt by human exposed to extreme heat wave in a complex urban area using a WRF-MENEX model, Int. J. Biometeorol. (2019), https://doi.org/10.1007/s00484-019-01705-1.

[7] D.D. Milošević, S. m. Savić, V. Marković, D. Arsenović, I. Šećerov, Outdoor human thermal comfort in local climate zones of Novi Sad (Serbia) during heat wave period, Hungarian Geogr. Bull. 65 (2016) 129–137, https://doi.org/10.15201/hungeobull.65.2.4.

[8] G.R. Roshan, A.A. Ghanghermeh, Q. Kong, Spatial and temporal analysis of outdoor human thermal comfort during heat and cold waves in Iran, Weather Clim. Extrem. 19 (2018) 58–67, https://doi.org/10.1016/j.wace.2018.01.005.

[9] F. Salata, I. Golasi, V. Ciancio, F. Rosso, Dressed for the season: clothing and outdoor thermal comfort in the Mediterranean population, Build. Environ. 146 (2018) 50–63, https://doi.org/10.1016/j.buildenv.2018.09.041.

[10] A. Tseliou, I.X. Tsiros, M. Nikolopoulou, Seasonal differences in thermal sensation in the outdoor urban environment of Mediterranean climates - the example of Athens, Greece, Int. J. Biometeorol. (2017) 1–18, https://doi.org/10.1007/s00484-016-1298-5.

[11] P. Cohen, O. Potchter, A. Matzarakis, Human thermal perception of Coastal Mediterranean outdoor urban environments, Appl. Geogr. 37 (2013) 1–10, https://doi.org/10.1016/J.APGEOG.2012.11.001.

[12] D. Founda, M. Santamouris, Synergies between urban heat island and heat waves in Athens (Greece), during an extremely hot summer, Sci. Rep. 7 (2012) 1, https://doi.org/10.1038/s41598-017-11407-6 2017.

[13] P. Ramamurthy, M. Sangobanwo, Inter-annual variability in urban heat island intensity over 10 major cities in the United States, Sustain. Cities Soc. 26 (2016) 65–75, https://doi.org/10.1016/j.scs.2016.05.012.

[14] D. D'Ippoliti, P. Michelozzi, C. Marino, B. Menne, M. Gonzales Cabre, K. Katsouyanni, S. Medina, A. Paldy, H.R. Anderson, F. Ballester, L. Bisanti, A. Peters, C.A. Perucci, The impact of heat waves on mortality in 9 European cities, 1990-2004, Epidemiology 19 (2008) S286–S287.

[15] D. Li, E. Bou-Zeid, D. Li, E. Bou-Zeid, Synergistic interactions between urban heat islands and heat waves: the impact in cities is larger than the sum of its parts*, J. Appl. Meteorol. Climatol. 52 (2013) 2051–2064, https://doi.org/10.1175/JAMC-D-13-02.1.

[16] P. Ramamurthy, D. Li, E. Bou-Zeid, High-resolution simulation of heatwave events in New York City, Theor. Appl. Climatol. 128 (2017) 89–102, https://doi.org/10.1007/s00704-015-1703-8.

[17] K. Ward, S. Lauf, B. Kleinschmit, W. Endlicher, Heat waves and urban heat islands in Europe: a review of relevant drivers, Sci. Total Environ. (2016) 569–570, https://doi.org/10.1016/j.scitotenv.2016.06.119 527–539.

[18] L. Malys, M. Musy, C. Inard, Microclimate and building energy consumption: study of different coupling methods, Adv. Build. Energy Res. 9 (2015) 151–174, https://doi.org/10.1080/17512549.2015.1043643.

[19] R. Evins, V. Dorer, J. Carmeliet, Simulating external longwave radiation exchange for buildings, Energy Build. 75 (2014) 472–482, https://doi.org/10.1016/J.ENBUILD.2014.02.030.

[20] S. Porritt, L. Shao, P. Cropper, C. Goodier, Adapting dwellings for heat waves, Sustain. Cities Soc. 1 (2011) 81–90, https://doi.org/10.1016/j.scs.2011.02.004.

[21] J. Zuo, S. Pullen, J. Palmer, H. Bennetts, N. Chileshe, T. Ma, Impacts of heat waves and corresponding measures: a review, J. Clean. Prod. 92 (2015) 1–12, https://doi.org/10.1016/j.jclepro.2014.12.078.

[22] S. Savić, A. Selakov, D. Milošević, Cold and warm air temperature spells during the winter and summer seasons and their impact on energy consumption in urban areas, Nat. Hazards 73 (2014) 373–387, https://doi.org/10.1007/s11069-014-1074-y.

[23] S. Magli, C. Lodi, L. Lombroso, A. Muscio, S. Teggi, Analysis of the urban heat island effects on building energy consumption, Int. J. Energy Environ. Eng. 6 (2015) 91–99, https://doi.org/10.1007/s40095-014-0154-9.

[24] A. Pyrgou, V.L. Castaldo, A.L. Pisello, F. Cotana, M. Santamouris, On the effect of summer heatwaves and urban overheating on building thermal-energy performance in central Italy, Sustain. Cities Soc. 28 (2017) 187–200, https://doi.org/10.1016/J.SCS.2016.09.012.

[25] M. Davies, P. Steadman, T. Oreszczyn, Strategies for the modification of the urban climate and the consequent impact on building energy use, Energy Policy 36 (2008) 4548–4551, https://doi.org/10.1016/j.enpol.2008.09.013.

[26] D. Founda, F. Pierros, M. Petrakis, C. Zerefos, Interdecadal variations and trends of the Urban Heat Island in Athens (Greece) and its response to heat waves, Atmos. Res. 161–162 (2015) 1–13, https://doi.org/10.1016/j.atmosres.2015.03.016.

[27] S. Falasca, G. Curci, Impact of highly reflective materials on meteorology, PM10 and ozone in urban areas: a modeling study with WRF-CHIMERE at high resolution over Milan (Italy), Urban Sci. 2 (2018) 18, https://doi.org/10.3390/urbansci2010018.

[28] S. Conti, P. Meli, G. Minelli, R. Solimini, V. Toccaceli, M. Vichi, C. Beltrano, L. Perini, Epidemiologic study of mortality during the Summer 2003 heat wave in Italy, Environ. Res. 98 (2005) 390–399, https://doi.org/10.1016/j.envres.2004.10.009.

[29] F. Salata, I. Golasi, R. de Lieto Vollaro, A. de Lieto Vollaro, Outdoor thermal comfort in the Mediterranean area. A transversal study in Rome, Italy, Build. Environ. 96 (2016) 46–61, https://doi.org/10.1016/j.buildenv.2015.11.023.

[30] D. Li, E. Bou-Zeid, M. Oppenheimer, The effectiveness of cool and green roofs as urban heat island mitigation strategies, Environ. Res. Lett. 9 (2014) 55002, https://doi.org/10.1088/1748-9326/9/5/055002.

[31] A. Synnefa, M. Santamouris, K. Apostolakis, On the development, optical properties and thermal performance of cool colored coatings for the urban environment, Sol. Energy 81 (2007) 488–497, https://doi.org/10.1016/j.solener.2006.08.005.

[32] D. Carvalho, H. Martins, M. Marta-Almeida, A. Rocha, C. Borrego, Urban resilience to future urban heat waves under a climate change scenario: a case study for Porto urban area (Portugal), Urban Clim. 19 (2017) 1–27, https://doi.org/10.1016/j.uclim.2016.11.005.

[33] E. Morini, A.G. Touchaei, F. Rossi, F. Cotana, H. Akbari, Evaluation of albedo enhancement to mitigate impacts of urban heat island in Rome (Italy) using WRF meteorological model, Urban Clim. 24 (2018) 551–566, https://doi.org/10.1016/j.uclim.2017.08.001.

[34] N. Zhang, Y. Chen, L. Luo, Y. Wang, Effectiveness of different urban heat island mitigation methods and their regional impacts, J. Hydrometeorol. 18 (2017) 2991–3012, https://doi.org/10.1175/jhm-d-17-0049.1.

[35] D. Ambrosini, G. Galli, B. Mancini, I. Nardi, S. Sfarra, Evaluating mitigation effects of urban heat islands in a historical small center with the ENVI-Met® climate model, Sustain 6 (2014) 7013–7029, https://doi.org/10.3390/su6107013.

[36] M. Žuvela-Aloise, K. Andre, H. Schwaiger, D.N. Bird, H. Gallaun, Modelling reduction of urban heat load in Vienna by modifying surface properties of roofs, Theor. Appl. Climatol. 131 (2018) 1005–1018, https://doi.org/10.1007/s00704-016-2024-2.

[37] F. Salata, I. Golasi, A.D.L. Vollaro, R.D.L. Vollaro, How high albedo and traditional buildings' materials and vegetation affect the quality of urban microclimate. A case study, Energy Build. 99 (2015) 32–49, https://doi.org/10.1016/j.enbuild.2015.04.010.

[38] F. Salata, I. Golasi, D. Petitti, E. de Lieto Vollaro, M. Coppi, A. de Lieto Vollaro, Relating microclimate, human thermal comfort and health during heat waves: an analysis of heat island mitigation strategies through a case study in an urban outdoor environment, Sustain. Cities Soc. 30 (2017), https://doi.org/10.1016/j.scs.2017.01.006.

[39] F. Salata, I. Golasi, E. de Lieto Vollaro, F. Bisegna, F. Nardecchia, M. Coppi, F. Gugliermetti, A.L. Vollaro, Evaluation of different urban microclimate mitigation strategies through a PMV analysis, Sustain 7 (2015), https://doi.org/10.3390/su7079012.

[40] P.O. Fanger, Thermal comfort. Analysis and applications in environmental engineering., Therm. Comf. Anal. Appl. Environ. Eng, Danish Technical Press, Copenhagen (DA), 1970https://www.cabdirect.org/cabdirect/abstract/19722700268.

[41] F. Salamanca, A. Martilli, C. Yagüe, A numerical study of the Urban Heat Island over Madrid during the DESIREX (2008) campaign with WRF and an evaluation of simple mitigation strategies, Int. J. Climatol. 32 (2012) 2372–2386, https://doi.org/10.1002/joc.3398.

[42] Y. Wang, U. Berardi, H. Akbari, Comparing the effects of urban heat island mitigation strategies for Toronto, Canada, Energy Build. 114 (2016), https://doi.org/10.1016/j.enbuild.2015.06.046.

[43] H. Akbari, C. Cartalis, D. Kolokotsa, A. Muscio, A.L. Pisello, F. Rossi, M. Santamouris, A. Synnef, N.H. WONG, M. Zinzi, Local climate change and urban heat island mitigation techniques – the state of the art, J. Civ. Eng. Manag. 22

(2015) 1–16, https://doi.org/10.3846/13923730.2015.1111934.
[44] P.A. Mirzaei, Recent challenges in modeling of urban heat island, Sustain. Cities Soc. 19 (2015) 200–206, https://doi.org/10.1016/j.scs.2015.04.001.
[45] R. Levinson, H. Akbari, Potential benefits of cool roofs on commercial buildings: conserving energy, saving money, and reducing emission of greenhouse gases and air pollutants, Energy Effic. 3 (2010) 53–109, https://doi.org/10.1007/s12053-008-9038-2.
[46] S. Falasca, F. Catalano, M. Moroni, Numerical study of the daytime planetary boundary layer over an idealized urban area: influence of surface properties, anthropogenic heat flux, and geostrophic wind intensity, J. Appl. Meteorol. Climatol. 55 (2016) 1021–1039, https://doi.org/10.1175/JAMC-D-15-0135.1.
[47] A. Sharma, P. Conry, H.J.S. Fernando, A.F. Hamlet, J.J. Hellmann, F. Chen, Green and cool roofs to mitigate urban heat island effects in the Chicago metropolitan area: evaluation with a regional climate model, Environ. Res. Lett. 11 (2016) 1–15, https://doi.org/10.1088/1748-9326/11/6/064004.
[48] W.C. Skamarock, J.B. Klemp, J. Dudhi, D.O. Gill, D.M. Barker, M.G. Duda, X.-Y. Huang, W. Wang, J.G. Powers, A Description of the Advanced Research WRF Version 3, Natl. Cent. Atmos. Res. Boulder, CO, USA, 2008, p. 113, https://doi.org/10.5065/D6DZ069T.
[49] A. Martilli, A. Clappier, M.W. Rotach, MESOSCALE MODELS, (2002), pp. 261–304.
[50] S. Falasca, G. Curci, High-resolution air quality modeling: sensitivity tests to horizontal resolution and urban canopy with WRF-CHIMERE, Atmos. Environ. 187 (2018) 241–254, https://doi.org/10.1016/J.ATMOSENV.2018.05.048.
[51] T.R. Oke, H.A. Cleugh, Urban heat storage derived as energy balance residuals, Boundary-Layer Meteorol. 39 (1987) 233–245, https://doi.org/10.1007/BF00116120.
[52] F. Rosso, A.L. Pisello, F. Cotana, M. Ferrero, On the thermal and visual pedestrians' perception about cool natural stones for urban paving: a field survey in summer conditions, Build. Environ. 107 (2016) 198–214, https://doi.org/10.1016/j.buildenv.2016.07.028.
[53] L. Doulos, M. Santamouris, I. Livada, Passive cooling of outdoor urban spaces. The role of materials, Sol. Energy 77 (2004) 231–249, https://doi.org/10.1016/j.solener.2004.04.005.
[54] N.L. Alchapar, E.N. Correa, M.A. Cantón, Classification of building materials used in the urban envelopes according to their capacity for mitigation of the urban heat island in semiarid zones, Energy Build. 69 (2014) 22–32, https://doi.org/10.1016/j.enbuild.2013.10.012.
[55] S. Sen, J. Roesler, Aging albedo model for asphalt pavement surfaces, J. Clean. Prod. 117 (2016) 169–175, https://doi.org/10.1016/J.JCLEPRO.2016.01.019.
[56] F. Rosso, I. Golasi, V.L. Castaldo, C. Piselli, A.L. Pisello, F. Salata, M. Ferrero, F. Cotana, A. de Lieto Vollaro, On the impact of innovative materials on outdoor thermal comfort of pedestrians in historical urban canyons, Renew. Energy 118 (2018) 825–839, https://doi.org/10.1016/j.renene.2017.11.074.
[57] A.L. Pisello, F. Cotana, The thermal effect of an innovative cool roof on residential buildings in Italy: results from two years of continuous monitoring, Energy Build. 69 (2014) 154–164, https://doi.org/10.1016/j.enbuild.2013.10.031.
[58] F. Rosso, A.L. Pisello, V.L. Castaldo, M. Ferrero, F. Cotana, On innovative cool-colored materials for building envelopes: balancing the architectural appearance and the thermal-energy performance in historical districts, Sustain (2017), https://doi.org/10.3390/su9122319.
[59] F. Leal, W. Adamson, K. Dunk, R.M. Azeiteiro, U.M. Illingworth, F. Alves, Implementing Climate Change Adaptation in Cities and Communities: Integrating Strategies and Educational Approaches, Springer, 2016, https://doi.org/10.1007/978-3-319-28591-7.
[60] F. Rosso, A.L. Pisello, V.L. Castaldo, C. Fabiani, F. Cotana, M. Ferrero, W. Jin, New Cool Concrete for Building Envelopes and Urban Paving: Optics-Energy and Thermal Assessment in Dynamic Conditions, Energy Build, 2017, https://doi.org/10.1016/j.enbuild.2017.06.051.
[61] R. Levinson, H. Akbari, P. Berdahl, K. Wood, W. Skilton, J. Petersheim, A novel technique for the production of cool colored concrete tile and asphalt shingle roofing products, Sol. Energy Mater. Sol. Cells 94 (2010) 946–954, https://doi.org/10.1016/j.solmat.2009.12.012.
[62] K.L. Uemoto, N.M.N. Sato, V.M. John, Estimating thermal performance of cool colored paints, Energy Build. 42 (2010) 17–22, https://doi.org/10.1016/j.enbuild.2009.07.026.
[63] D. Deru, K. M.Field, D. Studer, K. Benne, B. Griffith, P. Torcellini, B. Liu, M. Halverson, D. Winiarski, M. Rosenberg, M. Yazdanian, J. Huang, U.S. Crawley, Department of Energy Commercial Reference Building Models of the National Building Stock, (2011) U.S. https://digitalscholarship.unlv.edu/renew_pubs/44.
[64] D.B. Crawley, J.W. Hand, M. Kummert, B.T. Griffith, Contrasting the capabilities of building energy performance simulation programs, Build. Environ. 43 (2008) 661–673, https://doi.org/10.1016/J.BUILDENV.2006.10.027.
[65] A. Foucquier, S. Robert, F. Suard, L. Stéphan, A. Jay, State of the art in building modelling and energy performances prediction: a review, Renew. Sustain. Energy Rev. 23 (2013) 272–288, https://doi.org/10.1016/j.rser.2013.03.004.
[66] NREL, EnergyPlus - Weather Data Official site, https://energyplus.net/weather, (2018) https://energyplus.net/weather.
[67] F. Salata, I. Golasi, N. Treiani, R. Plos, A. de Lieto Vollaro, On the outdoor thermal perception and comfort of a Mediterranean subject across other Koppen-Geiger's climate zones, Environ. Res. 167 (2018) 115–128, https://doi.org/10.1016/j.envres.2018.07.011.
[68] D. de la Paz, R. Borge, A. Martilli, Assessment of a high resolution annual WRF-BEP/CMAQ simulation for the urban area of Madrid (Spain), Atmos. Environ. 144 (2016) 282–296, https://doi.org/10.1016/j.atmosenv.2016.08.082.
[69] J. Fallmann, R. Forkel, S. Emeis, Secondary effects of urban heat island mitigation measures on air quality, Atmos. Environ. 125 (2016) 199–211, https://doi.org/10.1016/j.atmosenv.2015.10.094.
[70] C. Giannaros, A. Nenes, T.M. Giannaros, K. Kourtidis, D. Melas, A comprehensive approach for the simulation of the Urban Heat Island effect with the WRF/SLUCM modeling system: the case of Athens (Greece), Atmos. Res. 201 (2018) 86–101, https://doi.org/10.1016/j.atmosres.2017.10.015.
[71] A. Schneider, M.A. Friedl, D. Potere, Mapping global urban areas using MODIS 500-m data: new methods and datasets based on "urban ecoregions, Remote Sens. Environ. 114 (2010) 1733–1746, https://doi.org/10.1016/J.RSE.2010.03.003.
[72] I. Golasi, F. Salata, E. de Lieto Vollaro, M. Coppi, A. de Lieto Vollaro, Thermal perception in the mediterranean area: comparing the mediterranean outdoor comfort index (MOCI) to other outdoor thermal comfort indices, Energies 9 (2016) 1–16, https://doi.org/10.3390/en9070550.
[73] I. Golasi, F. Salata, E. de Lieto Vollaro, M. Coppi, Complying with the demand of standardization in outdoor thermal comfort: a first approach to the Global Outdoor Comfort Index (GOCI), Build. Environ. 130 (2018), https://doi.org/10.1016/j.buildenv.2017.12.021.
[74] J.C. Chang, S.R. Hanna, Air quality model performance evaluation, Meteorol. Atmos. Phys. 87 (2004) 167–196, https://doi.org/10.1007/s00703-003-0070-7.
[75] V. Ciancio, S. Falasca, I. Golasi, G. Curci, M. Coppi, F. Salata, Influence of input climatic data on simulations of annual energy needs of a building: EnergyPlus and WRF modeling for a case study in Rome (Italy), Energies (2018), https://doi.org/10.3390/en11102835.